Characterization of lightweight aerated mortars using waste-to-energy bottom ash (WtE-BA) as aerating agent

Manon Brossat, Elodie Prud'Homme, Maria Lupsea-Toader, Denise Blanc, Christine de Brauer

Characterization of lightweight aerated mortars using Waste-to-Energy Bottom Ash (WtE-BA) as aerating agent

Manon Brossat [a,b], Elodie Prud'homme [b], Maria Lupsea-Toader [a], Denise Blanc [a,*], Christine de Brauer [a]

[a] Univ Lyon, INSA Lyon, DEEP, EA7429, 69621 Villeurbanne, FRANCE

[b] Univ Lyon, INSA Lyon, MATEIS, UMR CNRS 5510, 69621 Villeurbanne FRANCE

***** corresponding author : denise.blanc@insa-lyon.fr

Abstract

The management of Waste-to-Energy Bottom Ash (WtE-BA), generated during the incineration of waste, poses a global challenge. Presently, the majority of WtE-BA is disposed of in landfills due to the lack of alternatives. Meanwhile, the construction industry remains the primary consumer of raw materials and significantly contributes to Greenhouse Gas Emissions. This study attempts to address these issues by utilizing the fine fraction of WtE-BA (< 2mm) as a raw material for aerated mortar production. Thanks to its metallic aluminum content, WtE-BA is utilized as an aerating agent. The study investigates how the quantities of water and WtE-BA, as well as its granulometric sub-fractions, impact the properties of the final product. An analysis of properties such as density, compressive strength, and thermal conductivity was conducted. Additionally, the environmental impact of each raw material (i.e. WtE-BA, cement and sand) was assessed through leaching tests and elemental content analysis enabling the determination of their individual contribution to the presence of trace elements in the produced mortars. The aforementioned properties are discussed using

microstructure and porosity analyses. The findings demonstrate that the quantity of water is a crucial factor in controlling the aeration of mortars, whereas the granulometry of the WtE-BA particles did not significantly affect their macro-properties. Furthermore, this study highlights that WtE-BA based mortars has the potential to exhibit better environmental and insulating performances than aerated mortar of equal density and strength. The differences in pore size and type between WtE-BA and aerated mortars can account for the variation in performance. Thus, WtE-BA proves to be an effective substitute for aerating agent in the production of aerated mortars.

Keywords:

Waste-to-Energy Bottom Ash, Aerated material, Lightweight, Cement mortar, Leaching, Porosity

1. Introduction

Municipal Solid Waste Incineration (MSWI) is a popular waste management method as it helps sanitize and reduce the volume of waste, while generating electricity or heat (Brunner and Rechberger, 2015). In Europe, more than 150 million tons (Mt) of waste are incinerated annually, resulting in over 20 Mt of Waste-to-Energy Bottom Ash (WtE-BA) (Eurostat, 2018). Even though WtE-BA can be used as a road base material, roughly 46% of WtE-BA is still being sent to landfills due to a lack of available outlets (Blasenbauer et al., 2020).

Meanwhile, construction industry is the biggest consumer of raw materials in Europe accounting for half of the total extracted materials. Indeed, up to 80% of concrete

volume is made of natural aggregates that need to be excavated from quarries, resulting in significant damage to the local ecosystem as well as erosion of coastal areas or riverbanks (Sonak et al., 2006; Collivignarelli et al., 2020). To decrease the environmental impact of construction materials, the IEA (2022) highly recommends using alternative secondary raw materials in concrete and mortar.

Waste-to-Energy Bottom Ash is a promising alternative to traditional raw materials in concrete and mortar. Indeed, WtE-BA has the adequate chemical composition, mineralogy, and granulometry to potentially replace both cement and aggregates (Lam et al., 2010). Using WtE-BA in cementitious materials can have significant environmental benefits. This includes reducing the amount of landfilled WtE-BA, which causes various environmental concerns, such as groundwater and soil pollution or methane emissions (Alderete et al., 2021; Bawab et al., 2021). Furthermore, this approach can help address the issue of raw materials scarcity, while its wide availability would generate economic gains, thanks to a reduced need of transportation and its lower price compared to natural aggregates (AMORCE, 2018).

Over the past decades, numerous studies have been performed on the use of WtE-BA as a secondary raw material to produce cement-based materials (Pera et al., 1997; Bertolini et al., 2004; Rübner et al., 2008; Li et al., 2012; Lynn et al., 2016; Blanc et al., 2018; Zhang et al., 2021). However, there has been a notable lack of research regarding the utilization of the fine fraction of WtE-BA, specifically particles below 2 mm which accounts for 30 to 40 % of the total WtE-BA mass (Šyc et al., 2018). The substantial specific surface area combined with the high content of pollutants (Chimenos et al., 1999; Šyc et al., 2018; Huber et al., 2019) leads to a significant leaching potential of the WtE-BA fine fraction, which could affect the

environmental performances of the cementious material. For instance, Loginova et al. (2019) found that the concentration of Cu and Zn was over five times higher in eluates from fractions under 0.2 mm compared to those above 2 mm. Eventhough, several researches suggest that cementitious matrix can effectively stabilize WtE-BA pollutants, only few have focused on the utilization of WtE-BA fine fraction in construction material (Batchelor, 2006; Lam et al., 2010; Tang et al., 2013; Xuan et al., 2018; Loginova et al., 2021; Singh et al., 2022; Liu et al., 2023).

Moreover, most of the previous studies have described the swelling of the matrix caused by the formation of pores and cracks, leading to the reduction of the mechanical strength of samples. This swelling is attributed to the presence of reducing metals in the WtE-BA, especially metallic aluminum, which are very unstable in alkaline media (Aubert et al., 2004). During setting, oxidation of Al^0 takes place as per reaction (1), resulting in the generation of H_2 that becomes trapped in the matrix, thereby forming pores. At industrial scale, aluminum powder is traditionally used as a pore-forming agent to produce aerated goods.

$$2Al + 2OH^- + 2H_2O \rightarrow 2AlO_2^- + 3H_2 \quad (1)$$

To limit the harmful impact of reducing metals on the mechanical properties of cementitious materials, several studies applied chemical or physical pretreatment on WtE-BA (Tang et al., 2014; Saikia et al., 2015). Some techniques were successful, but the pre-treatment step increases the environmental impact and the costs (Ferraris et al., 2009).

Other studies assessed the feasibility of using the Al oxidation phenomenon to produce aerated matrices using WtE-BA (Qiao et al., 2008; Wongkeo et al., 2012; Chen et al., 2014; Song et al., 2015; Lynn et al., 2016; Li et al., 2018). Mostly, they

have specifically focused on the production of autoclaved aerated concrete (AAC), where the entrapment of gas generated by the oxidation of Al is favored by the high pressure and temperature applied (Wongkeo et al., 2012; Song et al., 2015; Li et al., 2018). These studies found that WtE-BA can be utilized to create AAC with equivalent density, but greater compressive strength than traditional AAC (Song et al., 2015). However, the autoclaving process necessitates costly equipment and is highly energy-intensive (Shi et al., 2019). To minimize the environmental impact of the final product and to open up the broadest possible use of WtE-BA in cementitious materials, the current study opted not to use autoclaving. Few studies have explored the utilization of WtE-BA for producing lightweight material without the need for autoclaving (Qiao et al., 2008; Chen et al., 2014; Lynn et al., 2016). These methods have successfully generated low-density material. However, heavy treatments such as sintering and pelletization have been performed on WtE-BA and have not resulted in reaching the expected compressive strength (Chen et al., 2014; Lynn et al., 2016). To our knowledge, no study has been conducted on the production of non-autoclaved mortars using the fine fraction of WtE-BA.

The goal of the current study is double: (i) to capitalize on the rapid reaction rate of the fine fraction (< 2 mm) to fully replace the pore-forming agent without applying expensive treatment in aerated mortar and (ii) to assess the feasibility of stabilizing the pollutants of the fine fraction of WtE-BA within the solid matrix of mortar.

This work studies the impact of mix parameters including water ratio, WtE-BA quantity and WtE-BA treatment, on both macro and micro properties of aerated mortars. Preliminary experiments were conducted on cement pastes to evaluate the influence of mix parameters and the feasibility of replacing the aerating agent by WtE-BA (Brossat et al., 2022). It was shown that the fine fraction of WtE-BA is

suitable to produce lightweight material, although optimizing the mix parameters is necessary to achieve satisfactory mechanical performance. Parameters that proved optimal at cement paste scale were applied at mortar scale for the production of aerated mortars using WtE-BA without further processing. Mechanical strength, insulation and environmental performances were evaluated. Specifically, the contribution of each raw material to the presence of pollutants is assessed in order to accurately distinguish the effect of WtE-BA. Characterization tools such as XRD or Mercury Porosimeter enabled to put in perspective results obtained at macroscopic scale. The current work is part of a three-steps project, whose final objective is the production of aerated concrete using the fine fraction of WtE-BA as aerating agent.

2. Materials & Methods

2.1. Raw materials

Portland cement 52.5 R from Lafarge (d = 3.10 $g.cm^{-3}$) and normalized sand (EN 196-1:2016) (d = 2.64 $g.cm^{-3}$) have been used in all mortar formulations.

The WtE-BA used in this study has been provided by the Zevo Malešice Incineration plant in Prague Czech Republic. This incineration plant produces more than 60 kt of WtE-BA per year. Raw WtE-BA (0 – 40 mm) undergoes magnetic separation on site. The studied samples were collected during 7 sampling campaigns from February to May 2021. Sieving at 2 mm and homogenization were performed by the Institute of Chemical Process Fundamentals in Prague. Only the WtE-BA fine fraction (WTE-BA FF) (< 2mm) has been used in this study. It has been dried for 1 week at 50 °C in a proofer, homogenized and stored in a cold room (+4±1 °C) to prevent further evolution of the matrix. Subsequent sieving has been performed using a Retsch AS

200 sieve shaker, to separate two subfractions of WtE-BA FF: the small fraction (0 – 0.1 mm) and medium fraction (0.1 – 0.25 mm). In addition, crushed WtE-BA have been obtained from WtE-BA FF using a ball mill with a speed of 450 rpm for 60 seconds. Crushing leads to a significant reduction of particles size with 92% of particles < 0.5 mm (against 50% in raw WtE-BA). A complete granulometric distribution of WtE-BA FF and crushed WtE-BA can be found in the *Supplementary material*.

Reducing metals (aluminum, zinc, etc content of WtE-BA FF has been determined by hydrogen generation in alkaline media. This protocol is widely described in literature (Aubert et al., 2004; Song et al., 2015; Wang et al., 2016)**.** Results are presented in Table 1. Elemental content of each raw material (i.e. WtE-BA, sand and cement) has been performed according to (Carignan et al., 2001) protocol in which powdered samples are fused with lithium metaborate $LiBO_2$ at high temperature and dissolved in a solution of nitric acid. Elemental quantification was performed using ICP-MS and ICP-OES. Major mineralogical phases of WtE-BA have been identified using Bruker Advance D8 X-ray Diffractometer. Results can be found in the *Supplementary material*. Densities of WtE-BA and traditional raw materials have been determined using a helium pycnometer Micrometrics Accupyc II.

Table 1 : Properties of WtE-BA fine fraction and sub-fractions used in this study

Denomination	Cz 0 – 2 (C)	Cz 0.1 – 0.2 (M)	Cz 0 – 0.1 (S)
Abbreviation	C (crushed)	M (medium)	S (small)
Particles size	< 0.50 mm after crushing	0.10 – 0.25 mm	0 – 0.10 mm
Proportion of the whole FF fraction	100%	14%	12%
Density ($g.cm^{-3}$)	2.59	2.48	2.44
Major oxides proportions (SiO_2 – CaO – Al_2O_3) (%)	37.8 – 18.5 – 11.6	28.0 – 23.1 – 12.1	16.9 – 27.4 – 12.5
Reducing metals content (%)	1.9	0.5	0.5
Time to react during quantification of reducing metals (min)	121	83	44

2.2. Cementitious materials production

Preliminary experiments have been performed using cement paste (made of Portland cement, WtE-BA and water) in order to assess the influence of different mix parameters such as: (i) water/binder ratio, (ii) WtE-BA amount, (iii) granulometric sub-fraction of WtE-BA and (iv) crushing of WtE-BA. Four levels per parameter have been tested (Brossat et al., 2022). A design of experiment based on Taguchi method has been implemented to define 16 representative formulations to be tested on mortars. For each parameter, compressive strength, swelling and density have been

assessed. Mix conditions are being considered as optimal if they enable the production of light and strong material. Best potential mix conditions have been implemented on mortars to proceed to an in-depth study of their properties.

Five mortar formulations using WtE-BA FF have been compared to two reference mortars. The two references are:

i. standard mortar produced according to EN 196-1: 2016 (further referred to as SM);

ii. aerated mortar (further called AM) in which 0.5 wt.% Al^0 powder (particles size < 45 µm and purity > 99.5% grade) is added.

The composition of each formulation is given in Table 2.

Table 2 : Mix proportions used for WtE-BA and reference mortars (standard mortar – SM – and aerated ortar – AM). Binder is here defined as the amount of cement and WtE-BA. Nomenclature of sample informs on W/B- Amount of IBA- fraction of WtE-BA

Samples (g)	SM	AM	0.4-Cz20S	0.55-Cz20S	0.55-Cz50S	0.55-Cz50M	0.55-Cz50C
Cement	450	450	450	450	450	450	450
Sand	1350	1350	1350	1350	1350	1350	1350
WtE-BA	-	-	90	90	225	225	225
Amount of WtE-BA *(%cement weight)*	-	-	20	20	50	50	50
Al powder *(%cement weight)*	-	0.5	-	-	-	-	-
Water/binder (W/B)	0.50	0.50	0.40	0.55	0.55	0.55	0.55

Due to its major oxides' proportions (rich in CaO and SiO_2) (see Table 1), WtE-BA is considered to take part in the development of hydrates. Therefore, the amount of binder in the water/binder (w/b) ratio is considered to be the sum of cement and WtE-BA amount. All samples have been produced according to the same protocol (adapted from EN 196-1: 2016, only mix proportions differ from the standard) and WtE-BA has been added at the same time as cement. Mortars have been casted and cured in 4x4x16 cm molds and stored under a protective sealing for 28 days before assessment.

2.3. Characterization tools and methods

Initial and final setting time have been assessed using standardized protocol (EN 196-3:2017). Bulk density of fresh and cured samples was determined by weight and volume measurements of the molds and performed in triplicate.

Mechanical strength has been assessed through flexural and compressive strength using a polyvalent tool for mechanical characterization from 3R Syntax with a speed of displacement of 1 $mm.s^{-1}$ and a maximal force of 100 kN according to EN 12390-4: 2019. Insulation properties were determined by thermal conductivity measurements after 28 days of curing. Measurements were performed during 80 s at 200 mW using a Hot Disk TP1500 with a Kapton probe of 9.9 mm. In order to evaluated as better as possible the actual operating conditions, no drying has been performed prior to these measurements.

A Mercury Intrusion Porosimetry (MIP) and X-ray tomography have been used to study the porosity of mortars. The MIP is a Micrometrics Autopore IV working from $3.47.10^{-3}$ to 398 MPa. It assesses the size distribution of porosities from 3 nm to 300 µm. Measurements have been performed in duplicate using several pieces of dried mortars of approximately 1 cm^3 in cells of 5 cm^3. In addition, X-Ray Tomography v|tome|x with a resolution of 25 µm combined with the software ImageJ have been used to observe the size, shape and geographical distribution of porosities above 25 µm. Acquisition was performed with an exposure time of 333 mS and 1200 points per samples (one point being the compilation of three images). This system also enables the determination of the proportion of volume occupied by pores measuring more than 50 µm (i.e. two times the resolution). This is done using a thresholding method to differentiate pores from the solid matrix. Tomography was performed on dried (at 50 °C for 48 hours) cylindrical samples of 3 cm diameter and up to 7 cm high

prepared using the same mortar batch as the rest of the study. The combination of MIP and tomography enables the complete determination of the volume of porosity, shapes and distribution of pores in mortars.

In addition, Scanning Electron Microscope (SEM) TESCAN Vega 3 has been used to visualize the microstructure of studied mortars. The observations were performed using secondary electron under high vacuum, accelerating voltage of 10 kV and at a working distance of 10.00 mm.

Environmental performances have been assessed on crushed mortars according to the EN 12457-2:2002 standard. Results have been compared with raw WtE-BA leaching and threshold from the Dutch legislation (Soil Quality Decree, 2007 on unmolded material).

Calculation of saturation indices of mineral phases present in the LLNL database (using PhreeqC software) helped at understanding the leaching mechanisms. In addition, retention and contribution of each raw material has been assessed.

Retention was defined as the amount of an element that is retained in the solid matrix after leaching. It is calculated with respect to the initial amount of this element in mortars and the leached amount. For a given element “el” it is calculated using formula (2):

$$Retention = \frac{m_{el\_m} - m_{el\_leached}}{m_{el\_m}} \quad (2)$$

With $m_{eL\_leached}$ the mass of element leached by a specified mass of mortar and m_{el_m} the initial element mass in mortar. Where m_{el_m} is defined as follows in (3):

$$m_{el\_m} = \frac{\sum_i w_{el\_i} * m_i}{m_m} \quad (3)$$

Where w_{el_i} is the mass fraction of the element in the raw material *i*, expressed in µg/g ; m_i the mass of raw material *i* introduced in the mortar and m_m the total mass of mortar.

3. Results and discussions

3.1. Cement pastes

Figure 1(a) and Figure 1(b) display the diagrams of effect of the mix proportions on compressive strength and bulk density respectively. Swelling, has been assessed visually and is supposed to be correlated with porosity and density. Therefore, the latter two will not be further discussed at this scale. These results have been throughly discussed in Brossat et al. (2022).

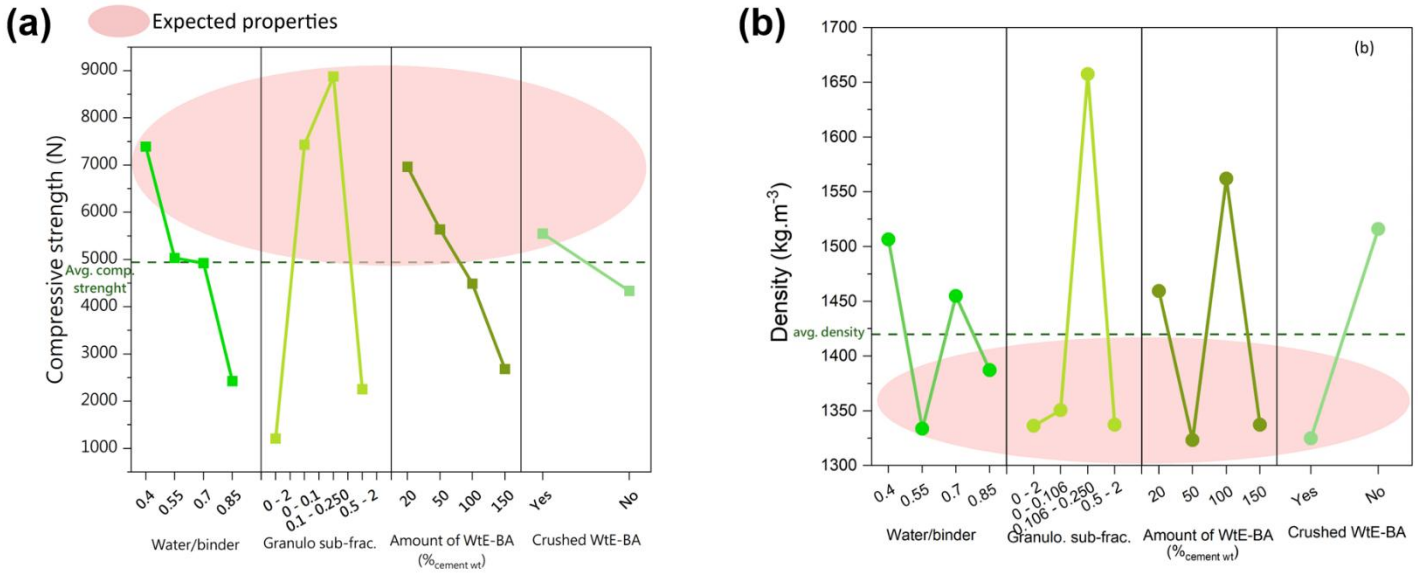

Figure 1 : Diagram of effect on (a) compressive strength and (b) density (Brossat et al., 2022)

The aim is to reach low density and high compressive strength. However, these properties are described as proportional meaning that low density is usually correlated with low mechanical strength (Hoff, 1972). In this study, if no compromise can be found, the development of compressive strength is favored.

Water/binder ratio (w/b) of 0.55 and 0.85 seem to be the most promising to reach low density, while w/b = 0.40 shows a high compressive strength. The compressive strength of formulations with a w/b = 0.85 is however too low to be carried out at larger scale. Therefore, w/b of 0.40 and 0.55 are considered to be adequate and will be used at mortar scale.

Granulometric sub-fractions 0 – 2 mm, 0.5 – 2 mm and 0 – 0.1 mm show comparable density, but the compressive strength of the latter is much higher than the others. Despite its low mechanical properties, raw WtE-BA FF, namely sub-fraction 0 – 2 mm, will be implemented on mortar since its use does not imply additional treatment prior to incorporation. Regardless of the density, compressive strengths of

formulations using sub-fractions 0 – 0.1 mm (S) and 0.1 – 0.25 mm (M) are very high compared to other mix parameters, and will therefore be tested on mortars.

The increase of WtE-BA amount leads to a steadily decrease of compressive strength. On the other hand, no trend can be identified on the impact of WtE-BA amount on density. Therefore, to maximise the mechanical performances only the formulations using 20% and 50% of WtE-BA will be tested on mortars.

Finally, the crushing of WtE-BA is beneficial to both density and compressive strength. However, further experiments showed that crushing of the sub-fractions S and M does not reduce significantly their particle size. To reduce the number of steps before incorporating WtE-BA and to avoid unnecessary energy cost and handling, only raw WtE-BA is crushed in mortar samples.

3.2. Properties of mortars at fresh state

3.2.1. Setting time

Table 3 displays the properties at fresh state of mortars. The initial and final setting time tend to increase with the incorporation of any proportion of WtE-BA, except for 0.4-Cz20S (due to its lower w/b ratio). This observation is in accordance with previous results in literature (Trussell and Spence, 1994; Caprai et al., 2019). This delay is most likely due to the presence of residual organic matter in the WtE-BA(>14%, see *Supplementary Materials*). In fact, active organic matter can delay the setting by adsorbing the Ca^{2+} ions released during hydration. This slows down the formation of C-S-H which are only produced at high concentrations of Ca^{2+} (Bullard et al., 2011). In addition, the presence of soluble salts in the WtE-BA, such as chlorides, sulfates or nitrates, can lead to a delayed hydration (Caprai et al., 2019). The delay of initial setting time can be detrimental for the aeration of mortar. During the setting,

because of the thixotropic behavior of cement paste, and hardening of the matrix due to hydration mechanisms, the viscosity of the paste increases (Shaughnessy and Clark, 1988; Sun et al., 2017). Yet, viscosity is one of the main parameters governing the capturing of H_2 in the matrix and therefore the increase of the porosity of the sample. If the viscosity of the paste is too low while H_2 is generated, most of the produced gas cannot be entrapped in the matrix, and very few pores are formed. In addition, as explained by Wee et al. (2011) and Suleymanova et al. (2019), the development of pores in a fresh cement paste is mainly governed by the surface tension that is strongly linked to viscosity. This highlights the importance of the simultaneity of H_2 production and hardening of paste to obtain highly aerated mortar.

Table 3 : Properties at fresh state of mortar pastes

Samples	SM	AM	0.4-Cz20S	0.55-Cz20S	0.55-Cz50S	0.55-Cz50M	0.55-Cz50C
Initial setting time (min)	27	13	9	60	13	45	90
Final setting time (min)	130	155	30	260	113	420	600
Flow diameter (mm)	212 ±6	198 ±9	99 ±1	206 ±2	156 ±2	197 ±2	233 ±6
Density of fresh paste (kg/m^3)	2188 ±28.1	2191 ±28.2	1882 ±9.9	1923 ±1.6	1830 ±11.6	1786 ±23.1	2046 ±26.4
Density at 28 days (kg/m^3)	2178 ±39	1851 ±118	1913 ±67	1879 ±31	1765 ±33	1702 ±40	1762 ±18

3.2.2. Viscosity

It should be noted that no direct viscosity measurements have been made. Instead, viscosity is estimated from flow diameter measurements. Flow diameter (FD) of SM and AM is comparable and close to 205 mm (see Table 3). The 0.4-Cz20S sample has the smallest flow diameter (99 mm), while 0.55-Cz20S demonstrates a FD of 206 mm comparable to references. This suggests that, as expected, low w/b results in poor fluidity. The addition of WtE-BA decreases the fluidity of the paste since the FD of 0.55-Cz50S (156 mm) is significantly smaller than the one of 0.55-Cz20S.

Moreover, the particle size of WtE-BA seems to have a significant influence on the consistency. It seems that the use of small particles, related to a high surface area and important water intake, leads to a low fluidity of the paste. On the contrary, sample 0.55-Cz50C is produced using the largest WtE-BA fraction (< 0.5 mm) of this study and presents the largest flow diameter (233 mm).

Ultimately, it's obvious that the incorporation of WtE-BA influences the viscosity of the paste by the amount added or the particle size. However, it is interesting to observe that at equivalent FD, thus equivalent fluidity, formulations with WtE-BA show longer initial and final setting time. This highlights that WtE-BA interfere clearly with the hydration process through the presence of organic matter and soluble salts.

3.3. Density

When comparing fresh and 28 days density of WtE-BA mortars with the SM reference (see Table 3), it is obvious that the addition of WtE-BA leads to a decrease of density supporting the hypothesis that WtE-BA can be used to produce lightweight mortars. At fresh state, all WtE-BA mortars have lower density than AM and SM, whereas after 28 days, WtE mortars are lighter than SM, but comparable to AM.

The lightness of WtE-BA mortars at fresh state can be explained by the low density of WtE-BA (< 2.59 $g.cm^{-3}$ for all sub-fractions) compared to the other components (cement density = 3.10 $g.cm^{-3}$ and sand = 2.65 $g.cm^{-3}$). Therefore, increasing the amount of WtE-BA in the formulations leads to a decrease in the fresh density as observed for the formulations 0.55-Cz20S (1923 ± 1.6 $kg.m^{-3}$) and 0.55-Cz50S (1830 ± 11.6 $kg.m^{-3}$). As the amount of WtE-BA increases, a decrease in 28-day density is also observed. This can be attributed to the increase in aluminum content caused by the increase in WtE-BA amount. In fact, previous studies have shown that the

number and volume of pores are proportional to the amount of metallic aluminum (Cabrillac et al., 2006; Tang Van et al., 2019). Therefore, increasing the amount of WtE-BA (which contains metallic aluminum – see) should result in higher porosity and lower density after curing. This explains the highest decrease in density of 0.55-Cz50S than 0.55-Cz20S between fresh and cured state.

At fresh state, bulk density is not only impacted by the amount of WtE-BA but also by its treatment (crushed or sieved), whereas it is not at 28 days. The use of crushed WtE-BA limits the reduction of the bulk density of fresh paste due to its higher density compared to sieved WtE-BA. After curing, thanks to a higher amount of Al^0 in crushed WtE-BA (see Table 1), density of 0.55-Cz50C samples decreased until reaching a density equivalent to formulations using sieved WtE-BA. This evolution of density through time demonstrates a proper aeration of the sample. This can be explained by a long setting time, in conjunction with WtE-BA oxidation, and proper viscosity enabling a good entrapment of H_2 produced during Al oxidation. On the other hand, only a small variation is observed between density at fresh and cured states of samples 0.55-Cz50S and 0.55-Cz50M, implying a poor entrapment of gas.

From Table 3, it seems that the increase of water amount leads to a slight increase in the density at fresh state (from 1882 ± 9.9 $kg.m^{-3}$ for 0.4-Cz20S to 1923 ± 1.6 $kg.m^{-3}$ for 0.55-Cz20S). Only a small variation is observed between the fresh and cured state of 0.4-Cz20S, implying that little aeration has occurred. This is consistent with the results of previous studies and can be related to the low viscosity of the paste and its rapid curing, thus limiting the entrapment of H_2 (Kim et al., 2014). On the contrary, there is a significant drop of density between fresh and cured state of sample 0.55-Cz20S demonstrating that a proper aeration occurred. This supports the

claim of Wee et al. (2011) and Pinilla Melo et al. (2014) that increasing the amount of water tends to decrease the yield stress of the fresh paste and favors pore formation.

3.4. Porosity

Evaluation of porosity is an interesting tool to understand the properties of mortars at macro-scale such as density, mechanical strength or thermal conductivity (Ganjian, 1990; Lian et al., 2011; Sun et al., 2017; Baranova et al., 2022).

Table 4 displays porosities obtained by the analysis of tomography images and MIP. Results on porosity will be treated apart, divided into macro-scale (obtained using X-ray tomography) and micro-scale (using MIP) observations. In addition, calculation of the overall porosity has been performed by combining results obtained using MIP and X-ray tomography.

Table 4 : Volume of porosity (in % of the total volume of sample) assessed using tomography (pores > 50µm) combined with the threshold method and Mercury Intrusion Porosimetry for pores between 0.003 µm and 300 µm

Samples	SM	AM	0.4-Cz20S	0.55-Cz20S	0.55-Cz50S	0.55-Cz50M	0.55-Cz50C
Volume of porosity (> 50 µm) by Tomography (%)	3.8	31.8	3.8	8.1	7.7	14.4	10.1
Volume of porosity [0.003-300 µm] by MIP (%)	13.1	21.8	29.6	36.5	27.0	29.9	18.4
Estimation of the total volume of porosity (%)	15.8±0.3	42.7±1.5	31.1±0.6	42.1±0.6	32.6±0.3	41.8±0.6	26.5±0.3

3.4.1. Macro-scale study of the porosity using tomography (> 50 µm)

At macroscale, as anticipated, SM exhibits the lowest porosity (3.8%, equivalent to the porosity of 0.4-Cz20S). Its porosity is over eight times smaller than that of AM (31.8%), which is the most porous sample. The macro-porosity of WtE-BA mortars ranges from 3.8% for sample 0.4-Cz20S to 14.4% for 0.55-Cz50M, which is about twice as low as the macro-porosity of AM. The comparison of porosities among the

three formulations using the S sub-fraction shows that an increase in water content leads to the increase of porosity, potentially related to optimal flowability (see Table 3). On the other hand, the addition of WtE-BA does not affect significantly the porosity.

The treatment on the WtE-BA used (crushed or sieved) seems to influence the development of the amount and shape of macro-porosity. For instance, mortar 0.55-Cz50S is about 2 times less porous than the formulation containing M sub-fraction. This finding is unexpected since WtE-BA sub-fractions S and M have a comparable content of reactive metals and an equivalent time of reaction (see Table 1), but may be explained by their different behavior at fresh state. Indeed, the lower flowability and setting time of 0.55-Cz50S present a fast increase in viscosity, thus limiting the potential development of big pores. In addition, sample 0.55-Cz50C exhibits an intermediate macroporosity of 10.1%, the highest concentration in reducing metals and the greatest flowability and setting time. These results indicate that an optimum level of flowability and setting time must be achieved without exceeding these parameters to obtain maximum porosity. Figure 2 displays cross-sections of mortars obtained by tomography and ImageJ toolbox.

The images in Figure 2 highlight the presence of 2 kinds of pores in mortars:

i. small spherical pores (with a diameter inferior to 1 mm) that are mostly gathered around grains and are due to water evaporation (Schober, 2011), that can be clearly observed in SM (see Figure 2(a)) and
ii. larger and rather irregular pores, also called air pores, similar to those observed in AM (see Figure 2(b)). The irregular shape results from the coalescence of small pores, leading to the formation of larger ones. Pores measuring more than 100 µm

are referred to as ‘air pores’ in literature and are caused by the oxidation of reducing metals (Schober, 2011).

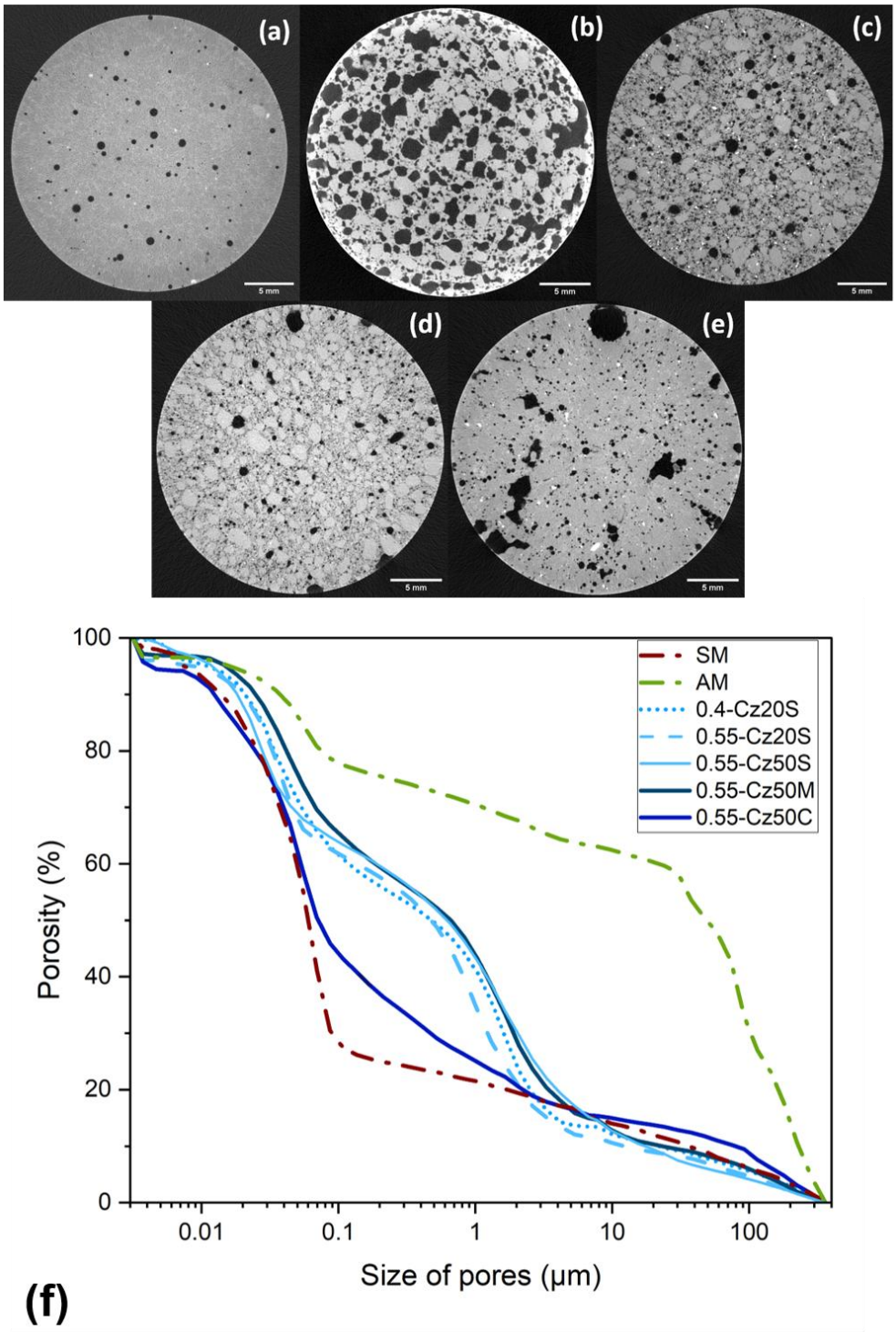

Figure 2 : Tomography of mortars performed on cylindrical samples of 3 cm diameter and 7 cm high. Vox. Size v= 25 µm (a) SM (b) AM (c) 0.55-Cz50M (d) 0.55-Cz50S (e) 0.55-Cz50C. (f) Size distribution of pores measuring using MIP from 0.003 to 300 µm

The porosity features of WtE-BA mortars vary across different formulations – 0.55-Cz50C seams to have very irregular pores compared to 0.55-Cz50S and 0.55-Cz50M.

Nevertheless, both types of pores are present in all WtE-BA mortars.

Tomography is also useful to distinguish materials of different densities. For example, grains of standardized sand are clearly distinguishable in Figure 2(d), for sample 0.55-Cz50S. This demonstrates a generally low-density matrix despite the few visible pores. In contrast, sample 0.55-Cz50C (Figure 2(e)) presents a solid and uniform matrix where distinguishing sand from the rest of the matrix is challenging. These differences between samples could be partly explained by the slight difference in density of granulometric sub-fractions S and M, that are lighter, compared to crushed WtE-BA and sand. Furthermore, micro-porosities cannot be observed distincly by tomography because of their size. However their presence affects how the density of the solid matrix is percevied on the tomograph.

3.4.2. Micro-scale study of the porosity using MIP

MIP has been used to assess the distribution of pores size from 0.003 to 300 µm. This technique has some limitations when used on irregular pores especially on the type of pores called “ink-bottle” (Abell et al., 1999), as it can lead to an underestimation of large pores compensated by an overestimation of small one.

Figure 2(f) depicts the aggregated porosity of mortar from 0.003 to 300 µm. The volume of micro-porosity is displayed in Table 4.

At this scale, the most WtE-BA samples exhibit higher pore volumes compared to AM and SM. The pore size distribution can be separated in three zones: (i) wide porosities (< 20 µm), (ii) intermediate porosities (0.1 to 20 µm) and (iii) small porosities (> 0.1 µm). AM is mostly composed of wide porosities, due to entrapment of gas. Approximately 60% of its pores attainable through MIP measure more than 20 µm, whereas the same threshold represents only 10% of SM and WtE-BA mortars

pores. More than half of WtE-BA mortars pores are in the intermediate size range, while this is valid for only 20% of AM and SM pores volume. Porosities between 0.5 and 5 µm are described in literature as inter-crystal porosities, while pores measuring from 5 to 30 µm are caused by water evaporation (Schober, 2011). More than 70% of SM pores measure between 0.1 and 0.01 µm and are attributed to the presence of hydration products such as C-S-H or tobermorite (Schober, 2011). These types of pores account for approximately 30% of the volume of pores in WtE-BA mortars and less than 10% in AM.

The presence of such hydrates has been confirmed by SEM observations. Honeycomb-like C-S-H structures are visible on SM sample in Figure 3(a), whereas less organized C-S-H are seen in 0.55-Cz50M sample in Figure 3(b). Observations of 0.55-Cz50S sample (see Figure 3(c)) show C-S-H displaying honeycomb structures and some tobermorite crystals (Alexanderson, 1979; Arizzi and Cultrone, 2021). The

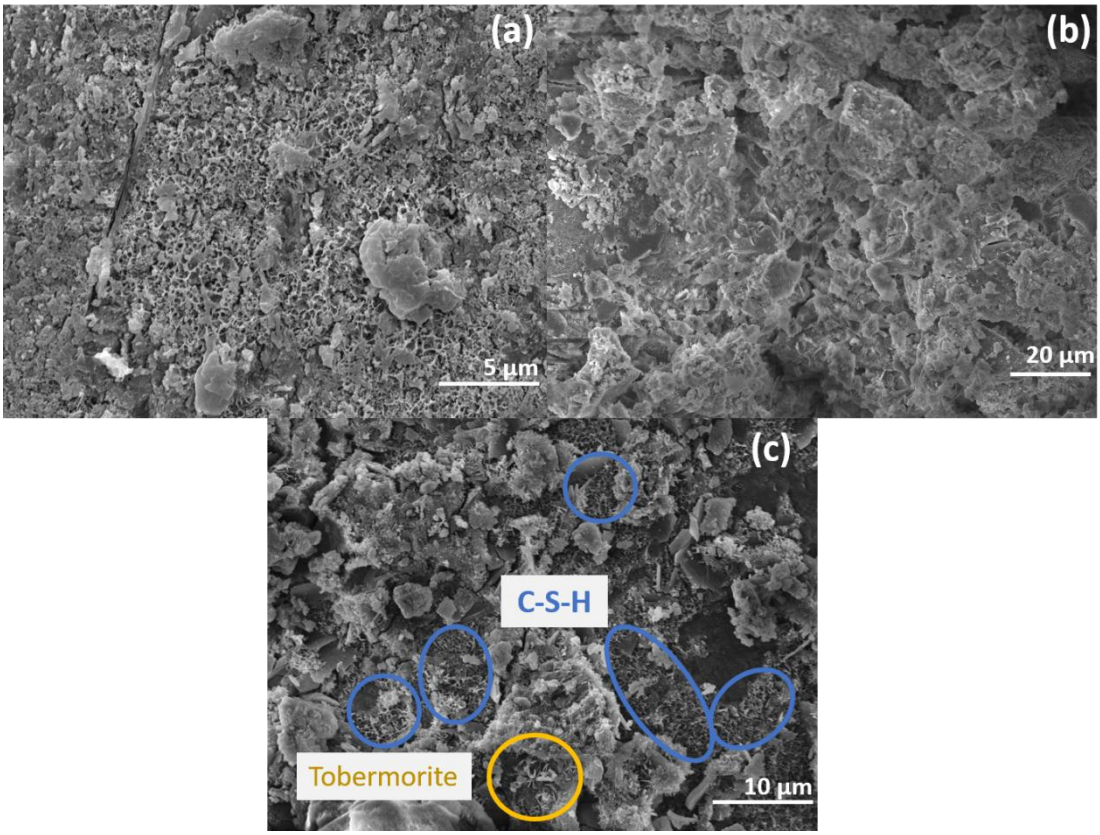

Figure 3 SEM observations (a) SM composed of honeycomb C-S-H (b) 0.55-Cz50M composed of disorganized C-S-H (c) 0.55-Cz50S with honeycomb C-S-H and some tobermorite crystals

pores of intermediate size observed in WtE-BA mortars in Figure 2 are described as the porosity of the ettringite network by Lo and Cui, (2004). However, only a few ettringite needles have been observed using SEM.

3.4.3. Study of the total porosity

By combining the results obtained using MIP and X-ray tomography, it is possible to evaluate the total volume of porosity measuring more than 0.003 µm. Due to the wide range (from 0.003 µm to few centimeters), the porosity obtained will be considered to be the total porosity.

SM is the less porous material with 15.8 ± 0.3% of its total volume made of pores. The result obtained using MIP is in line with literature (Kumar and Bhattacharjee, 2003). AM, along with samples 0.55-Cz20S and 0.55-Cz50M, are the most porous formulations with around 42% of porosity. The other formulations made with WtE-BA display intermediate porosity, 0.55-Cz50C being the least porous WtE-BA mortar with 26.5 ± 0.3% of pores.

This approach highlights the importance of the scale of study when assessing the porosity. Indeed, results show that samples highly porous at macro-scale are not necessarily porous at micro-scale, and conversely. An overall approach is necessary to assess precisely the porous structure of the cementitious materials. The study of sample 0.40-Cz20S is a good example of this observation as it is the least porous at macro-scale (3.8%), but still displays a total porosity of 31.1 ± 0.3%.

Contrary to what one would expect, the most porous samples are not necessarily the lightest. This emphasizes the significant role of the intrinsic density of raw materials to produce lightweight mortars.

3.5. Compressive strength

The results of compressive strength after 28 days of endogenous curing are presented in Figure 4.

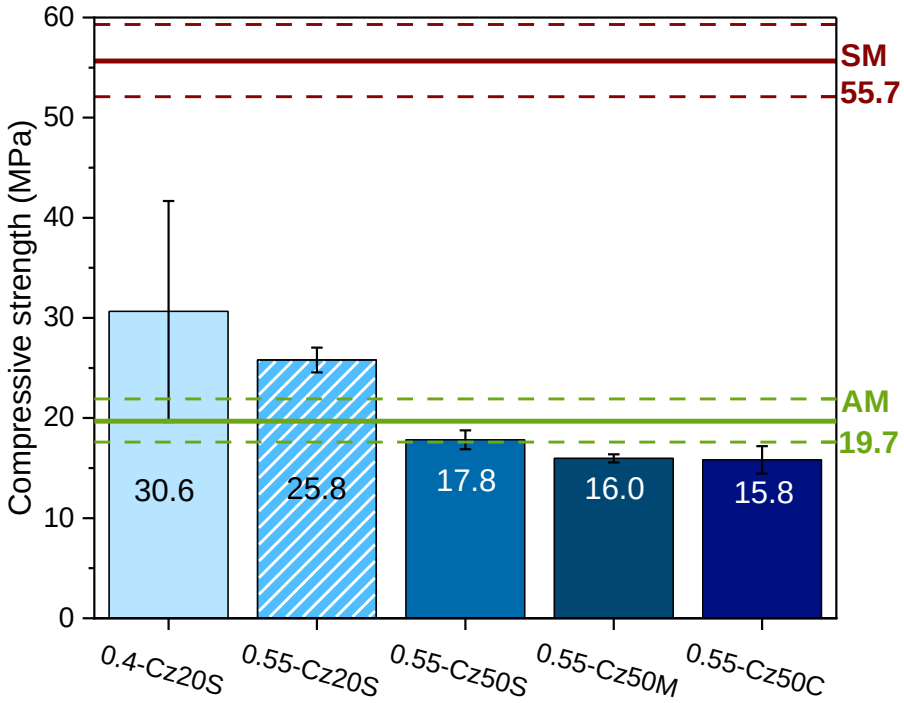

Figure 4 Effects of mix proportions on compressive strength of WtE-BA mortars compared with standardized and aerated mortars

As expected and in accordance with several results from literature, the compressive strength of all WtE-BA mortars is lower than the one of SM (Bertolini et al., 2004; Li et al., 2018; Caprai et al., 2019). However, compressive strength of WtE-BA mortars is superior or comparable to that of AM.

It seems that the amount of WtE-BA plays an important role in the development of mechanical properties of mortars, since the two samples containing 20% of WtE-BA show a higher compressive strength than the ones made with 50% of WtE-BA and AM. First, the addition of WtE-BA decreases the overall percentage of cement due to an increase in the paste volume (see Table 2). While WtE-BA does exhibit certain pozzolanic activity it appears inadequate in offsetting the loss caused by the reduction of the global proportion of cement (Cheng, 2012). Additionally, the extended setting time and reduced compressive strength suggest a potential

interaction between WtE-BA and hydration reactions. This interaction is clearly visible on SEM images, on which hydrates responsible for the development of compressive strength, such as C-S-H are less numerous and less organized in WtE-BA mortars than in SM(see Figure 3) . Also, as previously mentioned, the addition of WtE-BA causes an important porosity in the matrix especially in the range 0.003 to 300 µm, which can be detrimental to compressive strength (Alexanderson, 1979; Baranova et al., 2022).

Finally, samples 0.55-Cz50S, 0.55-Cz50M and 0.55-Cz50C show similar compressive strength, meaning that the treatment and particle size of bottom ash (i.e. crushed, sieved, S or M – see Table 1) has no influence on the development of mechanical strength. The close bulk density of the samples can explain the similar mechanical behavior (see Table 3). However, this is not consistent with the total porosity results – the three samples display different total porosities. As suggested by SEM observations, the strength lost due to porosity is compensated by the strength of the solid structure through the development of different types of hydrates (see Figure 3).

3.6. Thermal conductivity

Figure 5(a) depicts the thermal conductivity of the studied mortars. The same trend as compressive strength can be observed for thermal conductivity. Every formulation containing WtE-BA is more insulating than SM. Formulations using 20% of WtE-BA show an intermediate behavior to that of SM and AM, while formulations with 50% were found to be equal a more insulating than AM.

It seems that the addition of water is beneficial to achieve low thermal conductivity and may be related to the slight increase in small porosity observed in 0.55-Cz20S

compared to 0.40-Cz20S. Indeed, during the curing, some of the initial water is evaporated, leaving numerous capillaries and small porosities that are beneficial to reach good insulation properties (Schober, 2005).

As shown in Figure 5(b), there is a linear trend between density and thermal conductivity. This proportionality that has been described for lightweight aggregate concrete, is valid for WtE-BA mortars as well (Newman, 1993; Uysal et al., 2004; Real et al., 2016).

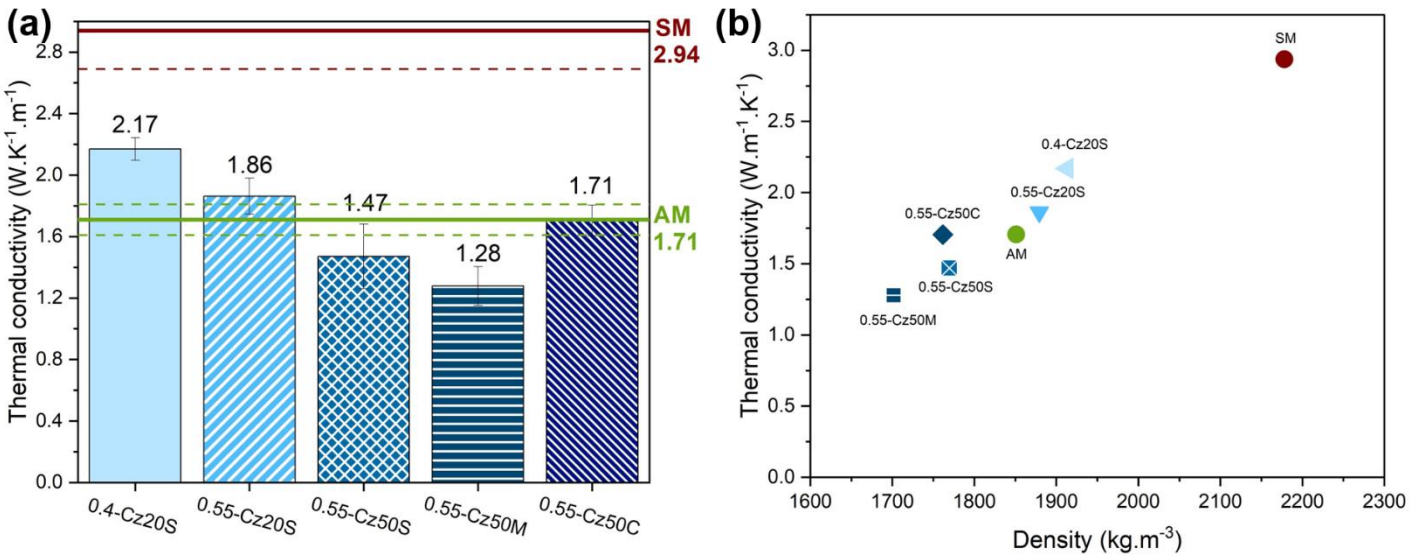

Figure 5 : Effects of mix proportions on thermal conductivity of WtE-BA mortars compared with standardized and aerated mortars (a) and correlation between thermal conductivity and bulk density of mortars (b).

Unlike compressive strength, some differences in thermal conductivity are observed between the formulations containing 50% WtE-BA. As observed in section 3.4, the different treatments of WtE-BA lead to various proportions, size distributions and

morphologies of pores in mortars. For instance, Chandra and Berntsson (2003) suggest that only porosities wider than 120 µm significantly influence thermal conductivity. This could explain why sample 0.55-Cz50M (with a macro-porosity of 14.4%) is slightly more insulating than 0.55-Cz50C (10.1%). However, this explanation fails to fully account for the behavior of bottom ash mortars. Although AM is the most porous mortar on a macroscopic scale, it is not the most insulating. Therefore, it appears the refinement of pores size, as suggested by Kreft et al. (2011), also contributes to the reduction of thermal conductivity.

This result is in accordance with previous studies who associated a high insulation potential with a high tortuosity and numerous separated pores (Schober, 2005, 2011; Wang and Dai, 2017).

The combination of small pores and light solid matrix might explain the interesting thermal behavior of 0.55-Cz50M. The lightness of 0.55-Cz50S solid matrix can also explain its relatively low thermal conductivity, whereas sample 0.55-Cz50C insulation properties seems to be linked to its porosity. In addition, despite the fact that sample 0.55-Cz20S demonstrates the highest volume of micro-porosities (36.5%) in this study, its thermal conductivity is relatively high (1.86 $W.m^{-1}.K^{-1}$) but consistent with the density of the sample (Figure 5**Erreur ! Source du renvoi introuvable.**Figure 5(b)).

It should be noted that all experiments were carried out on samples after 28 days of curing and without prior drying, in order to mimic real-life use conditions as closely as possible. The higher thermal conductivity of water ($\lambda \approx 0.598$ W $m^{-1}.K^{-1}$) in comparison to air ($\lambda \approx 0.026$ $W.m^{-1}.K^{-1}$) results in increased conductivity of humid samples when compared to dried ones (Uysal et al., 2004; Mohaine, 2018). This explains the high conductivity of presented samples, compared to litterature values.

3.7. Environmental performances

Leaching tests have been performed on ground mortars to comply with EN 12457-2:2002 standard. By grinding the mortars, the contact surface between the mortars and the leaching agent, and therefore the leaching of pollutants, is increased. Overestimation of leaching is acceptable, as it allows the worst-case scenario for environmental behavior.

Results for the leaching of several heavy metals and aluminum, and comparison to the Dutch SQD thresholds (*Soil Quality Decree*, 2007) for unmolded materials are presented in Figure 6. The Dutch thresholds have been used in this study due to lack of French and European legislation on the use of WtE-BA in construction material – other than as a road-based material.

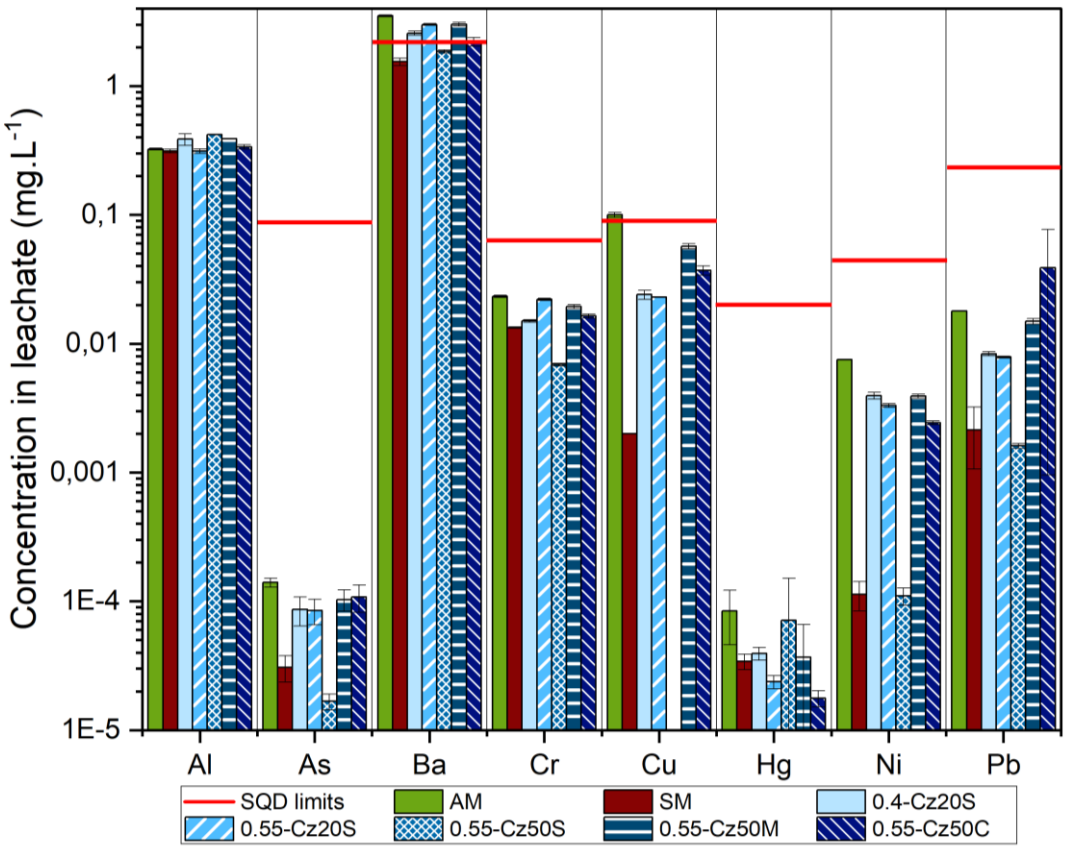

Figure 6 Effects of mix proportions on the leaching of WtE-BA mortars compared to SQD thresholds (Soil Quality Decree, 2007) and control mortars. Tests on ground mortars according to EN 12 457-2. For all samples Cd<9.0x10^{-6} mg.L^{-1}, Ti< 2.2x10^{-3} mg.L^{-1} and Zn< 1.0x10^{-3} mg.L^{-1}.

3.7.1. Comparison with legal limits

Figure 6 shows that all mortars, including or not WtE-BA, have a similar behavior and that no formulation clearly outstands. The concentration of pollutants in eluates doesn't exceed the SQD thresholds (*Soil Quality Decree*, 2007), except for Ba, for which 4 out of 7 formulations exceed the limit (including AM formulation and 3 WtE-BA mortars). In addition, the Cu threshold (0.054 g.L^{-1}) is exceeded by AM sample (0.1 g.L^{-1}).

For all samples, concentrations of Cd, Ti and Zn were below the detection limits, i.e. $9.0x10^{-6}$ $mg.L^{-1}$ for Cd, $2.2x10^{-3}$ $mg.L^{-1}$ for Ti and $1.0x10^{-3}$ $mg.L^{-1}$ for Zn.

Even if no Al threshold is defined in the SQD, its concentration in eluates was also measured to ensure that its addition (in the form of Al powder or WtE-BA) does not influence the leached amount. Leaching rates are equivalent among all samples and do not appear to be affected by either the quantity introduced into the mixture, or the form in which it was introduced. Calculating saturation indices of various phases from the LLNL database indicates that lawsonite ($CaAl_2Si_2O_7(OH)_2$-H_2O) is in equilibrium within the eluate. As a result, aluminum precipitation appears to be associated with a sorosilicate mineral phase.

The incorporation of WtE-BA appears not to be the primary factor affecting leaching since concentrations of leached elements are comparable for both formulations with and without WtE-BA. The high Pb concentration in 0.55-Cz50C could be explained by a nugget effect in one of its replicates.

On the whole, AM leaches the most, followed by 0.55-Cz50M. According to tomography analyses, AM and 0.55-Cz50M are also the most porous at macroscopic scale (see Table 4). The presence of porosity appears to be a significant factor in determining mortar leaching, as formulations containing a higher proportion of porosity exhibit more leaching than those with less porosity. This can be attributed to the increased surface area of porous samples. Although mortar grinding at 4 mm was conducted prior to leaching, this pre-treatment preserves the vast majority of macroscopic porosities.

3.7.2. Contribution of raw materials

Table 5 displays the contribution of each raw material to the total content of some elements of interest. Over the 10 elements of interest, WtE-BA is the main carrier for 4 of them, independently of the formulation (Al, Ba, Cd and Ti). Among the elements of interest, only As and Cr concentrations vary significantly from one sub-fraction to another. Arsenic content is decreasing as the particle size increases and is mostly carried by WtE-BA only in the mortar using the S sub-fraction. Cr content increases with the size of WtE-BA particles and WtE-BA becomes the first carrier when particle size increases.

Cement also contributes to the presence of trace elements (TE) in mortars, as it is the main supplier of Cu, Ni Pb and Zn. These results are in accordance with literature – due to co-incineration of waste in kiln, cement can bear various heavy metals (Müllauer et al., 2015; Horsley et al., 2016).

Table 5 Contribution of raw materials to the presence of TE in WtE-BA mortars using different WtE-BA sub-fractions

Element	0.55-Cz50S				0.55-Cz50M				0.55-Cz50C			
	Cement	Sand	WtE-BA	Total $\mu g/g_{mortar}$	Cement	Sand	WtE-BA	Total $\mu g/g_{mortar}$	Cement	Sand	WtE-BA	Total $\mu g/g_{mortar}$
Al	29%	11%	60%	6540	30%	11%	59%	6411	30%	12%	58%	6241
As	42%	10%	48%	3.14	47%	12%	41%	2.78	50%	12%	38%	2.62
Ba	7%	15%	77%	193	7%	16%	76%	184	8%	18%	74%	166.4
Cr	51%	12%	36%	14.7	45%	10%	45%	16.9	34%	8%	58%	22.2
Cd	5%	1%	94%	1.33	5%	1%	94%	1.25	10%	2%	88%	0.65
Cu	86%	12%	3%	9.71	86%	11%	3%	9.72	85%	12%	3%	9.75
Ni	86%	12%	2%	9.24	86%	12%	2%	9.25	86%	12%	2%	9.25
Pb	80%	16%	4%	8.33	80%	16%	4%	8.33	80%	16%	4%	8.38
Ti	19%	0%	81.1%	832	18%	0%	82%	891	20%	0%	80%	794
Zn	68%	9%	23%	45.1	73%	9%	18%	42.3	74%	9%	17%	41.7

3.7.3. Retention of pollutants

Based on the results of leaching and contribution of raw materials, the assessment of the retention of 17 elements (13 TE and 4 major elements) is possible. The extensive data can be found in the *Supplementary Materials*. The retention determines the proportion of elements that did not dissolve during leaching tests and are therefore still present in the solid matrix. For 11 out of the 17 studied elements, including Al, As, Cd, Fe, Ni, and Sb, retention is superior to 99% in all formulations and 16 elements have a retention of 90% or higher for all formulations including Cu, Cr or Pb. Barium is the only element showing a lower retention rate. WtE-BA is the primary source of Ba. As a results formulations containing WtE-BA are more enriched in this element.Nevertheless, these mortars exhibit a greater capacity for retaining barium than AM and SM. This observation is in accordance with (van der Sloot, 2002), who explains that Ba leaching is controlled by $BaSrSO_4$ and that, by adding waste, the leachability of sulfate is not following the ettringite-like phase pattern, leading to a better stabilization of $BaSrO_4$ in the solid matrix.

On the whole, the retention of pollutants is not affected by the incorporation of WtE-BA in mortars as it is within the range of AM and SM for all elements (except Pb, for which 0.55-Cz50C is the formulation that retains the least, but this was earlier attributed to a nugget effect).

4. Conclusion

The objective of this investigation was to utilize WtE-BA fine fraction as an aerating agent to generate mortars exhibiting characteristics akin to aerated mortar, while abstaining from the use of aerating agents. In order to evaluate properties of WtE-BA mortars, standardized and aerated mortars were produced as reference. The study

demonstrates that WtE-BA mortars can be lighter and more insulating than the intended aerated mortar, although they are less resistant. Microstructure analyses show that pores formed in WtE-BA mortars are generally smaller than pores found in aerated mortars and that this difference can partly explain the density, thermal and mechanical properties observed. In addition, the utilization of WtE-BA allows for a reduction in the density of mortars, even in the formulation with the lowest porosity. The environmental assessment demonstrates that WtE-BA incorporation does not change significantly the leaching mechanisms, except for barium which is more retained in WtE-BA mortars thanks to the stability of $BaSrSO_4$.

Finally, mix proportions are the key to obtain the expected properties. In this study, water amount is identified as the main parameter controlling viscosity of the fresh paste and hence, influencing the development of properties. The amount of WtE-BA seems to be of secondary importance in the range used in this study (from 20% to 50% of cement content), while the sub-fraction of WtE-BA has little to no effect on the compressive strength, thermal conductivity and density.

In order to deepen the understanding of the development of mechanical strength in WtE-BA mortars, future research could involve a study of the hydration rate and mechanisms in WtE-BA mortars. In addition, this study will be used as a preliminary step for the production of WtE-BA aerated concrete. Formulation using M sub-fraction has been found to be the most promising and will be carried out at concrete scale. The use of WtE-BA fine fraction (< 2 mm) in aerated concrete could highly reduce its material footprint, hence contributes to the transition of the construction industry to a more circular model.

Acknowledgment

The authors wish to acknowledge the financial support of the French Environment and Energy Management Agency ADEME, as part of ReFina project of the ERA-MIN network Nathalie Dumont and David Lebouil for the chemical analysis, Hervé Perrier-Camby, Richard Poncet, Jostar Lafôret and Jerôme Adrien for their experimental knowledge and help. Finally, authors would like to thank the SARM laboratory for their chemical analysis as well as ICPF and Pražské Služby for the sampling and providing the samples.

CRediT authorship contribution statement

Manon Brossat: Conceptualization, Methodology, Validation, Formal analysis, Investigation, Resources, Data Curation, Original Draft, Review & Editing, Visualization. **Elodie Prud'Homme:** Conceptualization, Methodology Validation, Resources, Data Curation, Review & Editing, Supervision, Project administration. **Maria Lupsea-Toader:** Conceptualization, Methodology, Review & Editing, Supervision, Project administration, Funding acquisition. **Denise Blanc:** Conceptualization, Methodology, Software, Validation, Review & Editing, Supervision, Project administration. **Christine de Brauer:** Conceptualization, Methodology, Validation, Review & Editing, Supervision, Project administration.

Declaration of Competing Interest

The authors declare that they have no competing financial interests or personal relationships that could have appeared to influence the work reported in this paper.

Funding

This work was developed within the Refina project supported by Era-Min network and was funded by Ademe agency (grant number 2002C0029).

References

Abell, A.B., Willis, K.L., Lange, D.A., 1999. Mercury Intrusion Porosimetry and Image Analysis of Cement-Based Materials. Journal of Colloid and Interface Science 211, 39–44. https://doi.org/10.1006/jcis.1998.5986

Alderete, N.M., Joseph, A.M., Van den Heede, P., Matthys, S., De Belie, N., 2021. Effective and sustainable use of municipal solid waste incineration bottom ash in concrete regarding strength and durability. Resources, Conservation and Recycling 167, 105356. https://doi.org/10.1016/j.resconrec.2020.105356

Alexanderson, J., 1979. Relations between structure and mechanical properties of autoclaved aerated concrete. Cement and Concrete Research 9, 507–514. https://doi.org/10.1016/0008-8846(79)90049-8

AMORCE, 2018. DT_92 Etats des lieux du recyclage des mâchefers en France.

Arizzi, A., Cultrone, G., 2021. Mortars and plasters—how to characterise hydraulic mortars. Archaeol Anthropol Sci 13, 144. https://doi.org/10.1007/s12520-021-01404-2

Aubert, J.E., Husson, B., Vaquier, A., 2004. Metallic aluminum in MSWI fly ash: quantification and influence on the properties of cement-based products. Waste Management 24, 589–596. https://doi.org/10.1016/j.wasman.2004.01.005

Baranova, A.A., Golubeva, A.O., Makarevich, O.S., Skulin, A.S., Kotsyr, A.Ig., 2022. Dependence of the strength characteristics of cellular concrete on their average density and porosity. Presented at the SiliconPV 2021, The 11th International Conference on Crystalline Silicon Photovoltaics, Hamelin, Germany / Online, p. 020001. https://doi.org/10.1063/5.0091554

Batchelor, B., 2006. Overview of waste stabilization with cement. Waste Management 26, 689–698. https://doi.org/10.1016/j.wasman.2006.01.020

Bawab, J., Khatib, J., Kenai, S., Sonebi, M., 2021. A Review on Cementitious Materials Including Municipal Solid Waste Incineration Bottom Ash (MSWI-BA) as Aggregates. Buildings 11, 179. https://doi.org/10.3390/buildings11050179

Bertolini, L., Carsana, M., Cassago, D., Curzio, A.Q., Collepardi, M., 2004. MSWI ashes as mineral additions in concrete. Cement and Concrete Research 8.

Blanc, D., Gonzalez, L., Lupsea-Toader, M., de Brauer, C., 2018. Mineralogical Evolution and Leaching Behaviour of a Heap of Bottom Ash as a Function of Time: Influence on Its Valorization. Waste Biomass Valor 9, 2517–2527. https://doi.org/10.1007/s12649-018-0444-1

Blasenbauer, D., Huber, F., Lederer, J., Quina, M.J., Blanc-Biscarat, D., Bogush, A., Bontempi, E., Blondeau, J., Chimenos, J.M., Dahlbo, H., Fagerqvist, J., Giro-Paloma, J., Hjelmar, O., Hyks, J., Keaney, J., Lupsea-Toader, M., O'Caollai, C.J., Orupõld, K., Pająk, T., Simon, F.-G., Svecova, L., Šyc, M., Ulvang, R., Vaajasaari, K., Van Caneghem, J., van Zomeren, A., Vasarevičius, S., Wégner, K., Fellner, J., 2020. Legal situation and current practice of waste incineration bottom ash utilisation in Europe. Waste Management 102, 868–883. https://doi.org/10.1016/j.wasman.2019.11.031

Brossat, M., Lupsea-Toader, M., Blanc, D., Prud'homme, E., de Brauer, C., 2022. Incorporation de la fraction fine de Mâchefers d'Incinération des Déchets Non-Dangereux (MIDND) dans des mortiers aérés.

Brunner, P.H., Rechberger, H., 2015. Waste to energy – key element for sustainable waste management. Waste Management 37, 3–12. https://doi.org/10.1016/j.wasman.2014.02.003

Bullard, J.W., Jennings, H.M., Livingston, R.A., Nonat, A., Scherer, G.W., Schweitzer, J.S., Scrivener, K.L., Thomas, J.J., 2011. Mechanisms of cement hydration. Cement and Concrete Research 41, 1208–1223. https://doi.org/10.1016/j.cemconres.2010.09.011

Cabrillac, R., Fiorio, B., Beaucour, A., Dumontet, H., Ortola, S., 2006. Experimental study of the mechanical anisotropy of aerated concretes and of the adjustment parameters of the

introduced porosity. Construction and Building Materials 20, 286–295. https://doi.org/10.1016/j.conbuildmat.2005.01.023

Caprai, V., Gauvin, F., Schollbach, K., Brouwers, H.J.H., 2019. MSWI bottom ash as binder replacement in wood cement composites. Construction and Building Materials 196, 672–680. https://doi.org/10.1016/j.conbuildmat.2018.11.153

Caractérisation des déchets - Lixiviation - Essai de conformité pour lixiviation des déchets fragmentés et des boues - Partie 2 : essai en bâchée unique avec un rapport liquide-solide de 10 l/kg et une granularité inférieure à 4 mm, 2002.

Carignan, J., Hild, P., Mevelle, G., Morel, J., Yeghicheyan, D., 2001. Routine Analyses of Trace Elements in Geological Samples using Flow Injection and Low Pressure On-Line Liquid Chromatography Coupled to ICP-MS: A Study of Geochemical Reference Materials BR, DR-N, UB-N, AN-G and GH. Geostandards and Geoanalytical Research 25, 187–198. https://doi.org/10.1111/j.1751-908X.2001.tb00595.x

Chandra, S., Berntsson, L., 2003. Lightweight aggregate concrete: science, technology. and applications. Noyes Publications, Norwich, N.J.

Chen, Z., Liu, Y., Yang, E.-H., 2014. Municipal Solid Waste Incineration Bottom Ash (IBA) As an Aerating Agent for the Production of Aerated Lightweight Concrete, in: ICSI 2014. Presented at the International Conference on Sustainable Infrastructure 2014, American Society of Civil Engineers, Long Beach, California, pp. 650–658. https://doi.org/10.1061/9780784478745.060

Cheng, A., 2012. Effect of incinerator bottom ash properties on mechanical and pore size of blended cement mortars. Materials & Design (1980-2015) 36, 859–864. https://doi.org/10.1016/j.matdes.2011.05.003

Chimenos, J.M., Segarra, M., Fernández, M.A., Espiell, F., 1999. Characterization of the bottom ash in municipal solid waste incinerator. Journal of Hazardous Materials 64, 211–222. https://doi.org/10.1016/S0304-3894(98)00246-5

Collivignarelli, M.C., Cillari, G., Ricciardi, P., Miino, M.C., Torretta, V., Rada, E.C., Abbà, A., 2020. The Production of Sustainable Concrete with the Use of Alternative Aggregates: A Review. Sustainability 12, 7903. https://doi.org/10.3390/su12197903

Essais pour béton durci - Partie 4 : résistance à la compression - Caractéristiques des machines d'essai, 2019.

Eurostat, 2018. Traitements des déchets en europe.

Ferraris, M., Salvo, M., Ventrella, A., Buzzi, L., Veglia, M., 2009. Use of vitrified MSWI bottom ashes for concrete production. Waste Management 29, 1041–1047. https://doi.org/10.1016/j.wasman.2008.07.014

Ganjian, E., 1990. The relationship between porosity and thermal conductivity of concrete. University of Leeds, UK.

Hoff, G.C., 1972. Porosity-strength considerations for cellular concrete. Cement and Concrete Research 2, 91–100. https://doi.org/10.1016/0008-8846(72)90026-9

Horsley, C., Emmert, M.H., Sakulich, A., 2016. Influence of alternative fuels on trace element content of ordinary portland cement. Fuel 184, 481–489. https://doi.org/10.1016/j.fuel.2016.07.038

Huber, F., Blasenbauer, D., Aschenbrenner, P., Fellner, J., 2019. Chemical composition and leachability of differently sized material fractions of municipal solid waste incineration bottom ash. Waste Management 95, 593–603. https://doi.org/10.1016/j.wasman.2019.06.047

IEA, 2022. Cement [WWW Document]. IEA. URL https://www.iea.org/reports/cement (accessed 2.16.23).

Kim, Y.-Y., Lee, K.-M., Bang, J.-W., Kwon, S.-J., 2014. Effect of W/C Ratio on Durability and Porosity in Cement Mortar with Constant Cement Amount. Advances in Materials Science and Engineering 2014, 1–11. https://doi.org/10.1155/2014/273460

Kreft, O., Hausmann, J., Hubálková, J., Aneziris, C.G., Straube, B., Schoch, T., 2011. Pore size distribution effects on the thermal conductivity of light weight autoclaved aerated concrete. Cement, Wapno, Beton 49–52.

Kumar, R., Bhattacharjee, B., 2003. Porosity, pore size distribution and in situ strength of concrete. Cement and Concrete Research 33, 155–164. https://doi.org/10.1016/S0008-8846(02)00942-0

Lam, C.H.K., Ip, A.W.M., Barford, J.P., McKay, G., 2010. Use of Incineration MSW Ash: A Review. Sustainability 2, 1943–1968. https://doi.org/10.3390/su2071943

Li, X., Liu, Z., Lv, Y., Cai, L., Jiang, D., Jiang, W., Jian, S., 2018. Utilization of municipal solid waste incineration bottom ash in autoclaved aerated concrete. Construction and Building Materials 178, 175–182. https://doi.org/10.1016/j.conbuildmat.2018.05.147

Li, X.-G., Lv, Y., Ma, B.-G., Chen, Q.-B., Yin, X.-B., Jian, S.-W., 2012. Utilization of municipal solid waste incineration bottom ash in blended cement. Journal of Cleaner Production 32, 96–100. https://doi.org/10.1016/j.jclepro.2012.03.038

Lian, C., Zhuge, Y., Beecham, S., 2011. The relationship between porosity and strength for porous concrete. Construction and Building Materials 25, 4294–4298. https://doi.org/10.1016/j.conbuildmat.2011.05.005

Liu, Y., Kumar, D., Lim, K.H., Lai, Y.L., Hu, Z., Ambikakumari Sanalkumar, K.U., Yang, E.-H., 2023. Efficient utilization of municipal solid waste incinerator bottom ash for autoclaved aerated concrete formulation. Journal of Building Engineering 71, 106463. https://doi.org/10.1016/j.jobe.2023.106463

Lo, T.Y., Cui, H.Z., 2004. Effect of porous lightweight aggregate on strength of concrete. Materials Letters 58, 916–919. https://doi.org/10.1016/j.matlet.2003.07.036

Loginova, E., Schollbach, K., Proskurnin, M., Brouwers, H.J.H., 2021. Municipal solid waste incineration bottom ash fines: Transformation into a minor additional constituent for

cements. Resources, Conservation and Recycling 166, 105354. https://doi.org/10.1016/j.resconrec.2020.105354

Loginova, E., Volkov, D.S., van de Wouw, P.M.F., Florea, M.V.A., Brouwers, H.J.H., 2019. Detailed characterization of particle size fractions of municipal solid waste incineration bottom ash. Journal of Cleaner Production 207, 866–874. https://doi.org/10.1016/j.jclepro.2018.10.022

Lynn, C.J., Dhir OBE, R.K., Ghataora, G.S., 2016. Municipal incinerated bottom ash characteristics and potential for use as aggregate in concrete. Construction and Building Materials 127, 504–517. https://doi.org/10.1016/j.conbuildmat.2016.09.132

Méthodes d'essai des ciments - Partie 3 : détermination du temps de prise et de la stabilité, 2017.

Méthodes d'essais des ciments - Partie 1 détermination des résistances, 2016.

Mohaine, S., 2018. Etude des propriétés thermiques et mécaniques des bétons isolants structurels incorporant des cénosphères (Génie Civil). Université Bretagne Loire - Centrale Nantes.

Müllauer, W., Beddoe, R.E., Heinz, D., 2015. Leaching behaviour of major and trace elements from concrete: Effect of fly ash and GGBS. Cement and Concrete Composites 58, 129–139. https://doi.org/10.1016/j.cemconcomp.2015.02.002

Newman, J., 1993. Properties of structural lightweight aggregate concrete, in: Structural Lightweight Aggregate Concrete. Chapman & Hall, Glasgow, UK, pp. 19–44.

Pera, J., Coutaz, L., Ambroise, J., Chababbet, M., 1997. Use of incinerator bottom ash in concrete. Cement and Concrete Research 27, 1–5. https://doi.org/10.1016/S0008-8846(96)00193-7

Pinilla Melo, J., Sepulcre Aguilar, A., Hernández Olivares, F., 2014. Rheological properties of aerated cement pastes with fly ash, metakaolin and sepiolite additions. Construction and Building Materials 65, 566–573. https://doi.org/10.1016/j.conbuildmat.2014.05.034

Qiao, X.C., Ng, B.R., Tyrer, M., Poon, C.S., Cheeseman, C.R., 2008. Production of lightweight concrete using incinerator bottom ash. Construction and Building Materials 22, 473–480. https://doi.org/10.1016/j.conbuildmat.2006.11.013

Real, S., da Gloria Gomes, M., Bogas, J.A., Ferrer, B., 2016. Thermal conductivity of structural lightweight aggregate concrete. Magazine of Concrete Research 68. https://doi.org/10.1680/jmacr.15.00424

Rübner, K., Haamkens, F., Linde, O., 2008. Use of municipal solid waste incinerator bottom ash as aggregate in concrete. Quarterly Journal of Engineering Geology and Hydrogeology 41, 459–464. https://doi.org/10.1144/1470-9236/07-036

Saikia, N., Mertens, G., Van Balen, K., Elsen, J., Van Gerven, T., Vandecasteele, C., 2015. Pre-treatment of municipal solid waste incineration (MSWI) bottom ash for utilisation in cement mortar. Construction and Building Materials 96, 76–85. https://doi.org/10.1016/j.conbuildmat.2015.07.185

Schober, 2005. The most important aspects of microstructure influencing strength of AAC. Presented at the 4th International Conference on Autocavec Aerated Concrete, Taylor and Francus, Kingston University-London, pp. 145–153.

Schober, G., 2011. Porosity in autoclaved aerated concrete (AA) : A review on pore structure, types of porosity, measurement methods and effects of porosity on properties 5.

Shaughnessy, R., Clark, P.E., 1988. The rheological behavior of fresh cement pastes. Cement and Concrete Research 18, 327–341. https://doi.org/10.1016/0008-8846(88)90067-1

Shi, Y., Li, Y., Tang, Y., Yuan, X., Wang, Q., Hong, J., Zuo, J., 2019. Life cycle assessment of autoclaved aerated fly ash and concrete block production: a case study in China. Environ Sci Pollut Res 26, 25432–25444. https://doi.org/10.1007/s11356-019-05708-8

Singh, A., Zhou, Y., Gupta, V., Sharma, R., 2022. Sustainable use of different size fractions of municipal solid waste incinerator bottom ash and recycled fine aggregates in cement mortar. Case Studies in Construction Materials 17, e01434. https://doi.org/10.1016/j.cscm.2022.e01434

Soil Quality Decree, 2007. , NL EN 200611115.

Sonak, S., Pangam, P., Sonak, M., Mayekar, D., 2006. Impact of sand mining on local ecology, in: Multiple Dimensions of Global Environmental Change.

Song, Y., Li, B., Yang, E.-H., Liu, Y., Ding, T., 2015. Feasibility study on utilization of municipal solid waste incineration bottom ash as aerating agent for the production of autoclaved aerated concrete. Cement and Concrete Composites 56, 51–58. https://doi.org/10.1016/j.cemconcomp.2014.11.006

Suleymanova, L.A., Pogorelova, I.A., Marushko, M.V., 2019. Theoretical Basis of Formation Highly Organized Porous Structure of Aerated Concrete. MSF 945, 309–317. https://doi.org/10.4028/www.scientific.net/MSF.945.309

Sun, Y., Gao, P., Geng, F., Li, H., Zhang, L., Liu, H., 2017. Thermal conductivity and mechanical properties of porous concrete materials. Materials Letters 209, 349–352. https://doi.org/10.1016/j.matlet.2017.08.046

Šyc, M., Krausová, A., Kameníková, P., Šomplák, R., Pavlas, M., Zach, B., Pohořelý, M., Svoboda, K., Punčochář, M., 2018. Material analysis of Bottom ash from waste-to-energy plants. Waste Management 73, 360–366. https://doi.org/10.1016/j.wasman.2017.10.045

Tang, P., Florea, M.V.A., Spiesz, P., Brouwers, H.J.H., 2014. The Application of Treated Bottom Ash in Mortar as Cement Replacement. Presented at the Proceedings of the EurAsia Waste Management Symposium 2014, 28-30 April 2014, Istanbul, Turkey Yildiz Technical University (YTU) and ISTAC Inc.., pp. 1077–1082.

Tang, P., Yu, Q.L., Yu, R., Brouwers, H.J.H., 2013. The application of MSWI bottom ash fines in high performance concrete. Presented at the 1st International Conference on the Chemistry of Construction Materials, Berlin, pp. 435–438.

Tang Van, L., Vu Kim, D., Ngo Xuan, H., Vu Dinh, T., Bulgakov, B., Bazhenova, S., 2019. Effect of Aluminium Powder on Light-weight Aerated Concrete Properties. E3S Web Conf. 97, 02005. https://doi.org/10.1051/e3sconf/20199702005

Trussell, S., Spence, R.D., 1994. A REVIEW OF SOLIDIFICATION/STABILIZATION INTERFERENCES 13.

Uysal, H., Demirboğa, R., Şahin, R., Gül, R., 2004. The effects of different cement dosages, slumps, and pumice aggregate ratios on the thermal conductivity and density of concrete. Cement and Concrete Research 34, 845–848. https://doi.org/10.1016/j.cemconres.2003.09.018

van der Sloot, H.A., 2002. Characterization of the leaching behaviour of concrete mortars and of cement–stabilized wastes with different waste loading for long term environmental assessment. Waste Management 22, 181–186. https://doi.org/10.1016/S0956-053X(01)00067-8

Wang, Y.-S., Dai, J.-G., 2017. X-ray computed tomography for pore-related characterization and simulation of cement mortar matrix. NDT & E International 86, 28–35. https://doi.org/10.1016/j.ndteint.2016.11.005

Wang, Z., Song, Y., Li, B., 2016. An Attempt to Reduce Materials Cost of Autoclaved Aerated Concrete Production. TOCIEJ 10, 323–333. https://doi.org/10.2174/1874149501610010323

Wee, T.-H., Daneti, S.B., Tamilselvan, T., 2011. Effect of w/c ratio on air-void system of foamed concrete and their influence on mechanical properties. Magazine of Concrete Research 63, 583–595. https://doi.org/10.1680/macr.2011.63.8.583

Wongkeo, W., Thongsanitgarn, P., Pimraksa, K., Chaipanich, A., 2012. Compressive strength, flexural strength and thermal conductivity of autoclaved concrete block made using bottom ash as cement replacement materials. Materials & Design 35, 434–439. https://doi.org/10.1016/j.matdes.2011.08.046

Xuan, D., Tang, P., Poon, C.S., 2018. Effect of casting methods and SCMs on properties of mortars prepared with fine MSW incineration bottom ash. Construction and Building Materials 167, 890–898. https://doi.org/10.1016/j.conbuildmat.2018.02.077

Zhang, S., Ghouleh, Z., He, Z., Hu, L., Shao, Y., 2021. Use of municipal solid waste incineration bottom ash as a supplementary cementitious material in dry-cast concrete. Construction and Building Materials 266, 120890. https://doi.org/10.1016/j.conbuildmat.2020.120890

Supplementary material

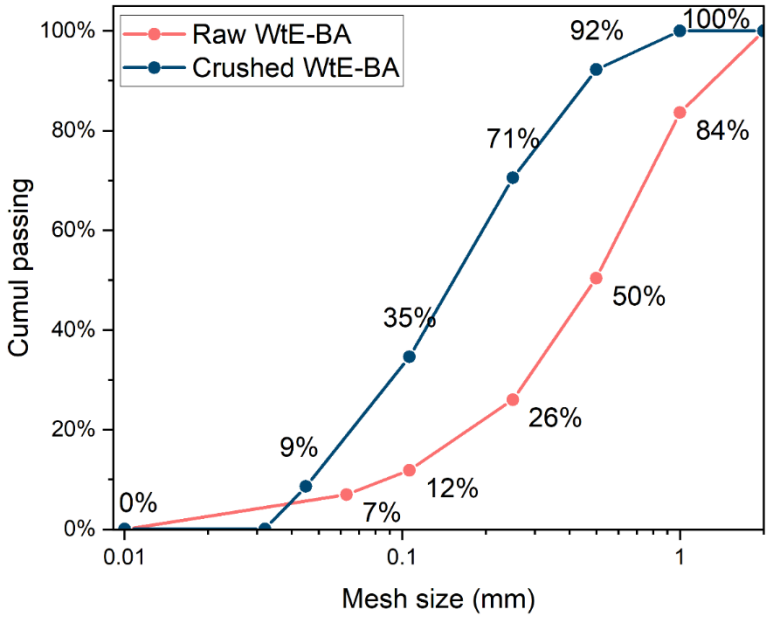

Figure S 1 Granulometric distribution of raw and crushed WtE-BA from Prague incinerator

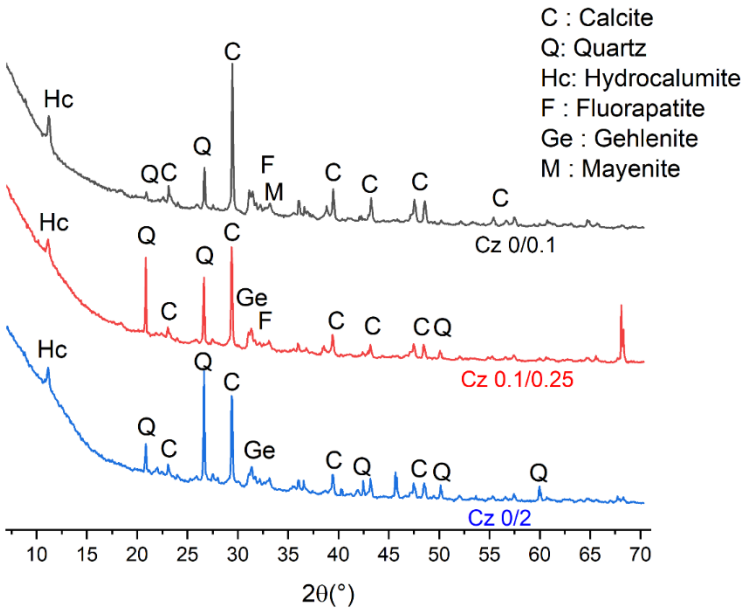

Figure S 2 Diffraction spectrum of different fractions of WTE-BA

Table S 1Major elements found in raw materials used in mortars

Oxides (%)	**Cement**	**Sand**	**Cz 0 – 2**	**Cz 0 – 0.1**	**Cz 0.1 – 0.25**
SiO_2	21.76	97.99	37.80	16.84	27.95
Al_2O_3	3.02	6.17	11.58	12.54	12.13
Fe_2O_3	2.26	0.03	7.84	3.21	4.95
MnO	0.073	< L.D.	0.17	0.18	0.14
MgO	0.71	< L.D.	1.64	1.91	1.81
CaO	64.38	< L.D.	18.49	27.43	23.14
Na_2O	0.10	< L.D.	2.54	1.97	2.33
K_2O	0.14	0.17	1.51	1.12	1.41
TiO_2	0.14	< L.D.	1.13	1.20	1.30
P_2O_5	< L.D.	< L.D.	2.01	2.04	2.39
PF	3.23	0.32	14.14	29.28	21.00

Table S 2 Elementary composition of raw materials in µg.g^{-1}

Elements (µg.g^{-1})	Cement	Sand	Cz 0 – 2	Cz 0 – 0.1	Cz 0.1 – 0.25
As	6.96	0,58	10.5	16.1	12.2
Ba	72.5	428	1309.7	1589.8	1496.8
Be	0.45	0.90	2.3	1.7	2.5
Bi	0.36	0.09	4.8	6.3	5.8
Cd	0.35	0.03	6.1	13.3	12.4
Co	3.57	1.78	42.6	37.2	40.1
Cr	40.3	8.7	136.8	56.8	80.6
Cs	0.50	1.38	374.8	403.8	356.7
Cu	44.4	4.3	3.1	2.7	2.8
Ga	3.70	5.80	2441.6	1271.4	1765.7
Ge	0.44	0.97	2.1	1.8	2.2
Hf	1.16	1.58	1.3	1.0	1.2
In	0.09	< L.D.	0.8	0.7	0.8
Mo	8.69	< L.D.	12.4	12.2	12.7
Nb	2.56	1.78	2.5	2.3	2.6
Ni	42.4	4.9	1.6	1.6	1.6
Pb	35.6	12.7	4.1	3.6	3.6
Rb	4.79	72.0	0.4	0.3	0.4
Sb	0.98	0.48	< L.D.	0.1	0.0
Sc	2.99	1.65	21.3	20.0	20.5
Sn	1.48	1.17	0.2	0.2	0.2
Sr	1258	66.8	9.4	11.2	10.4
Ta	0.24	0.24	15.9	12.5	15.8
Th	2.06	2.73	16.5	16.2	17.6
U	3.02	0.67	153.8	106.3	123.0
V	120	10.3	436.1	421.8	364.9
W	1.21	< L.D.	4.5	4.4	4.7
Y	11.0	5.43	32.9	22.5	28.3
Zn	163	16.0	75.6	111.8	82.3
Zr	44.2	56.5	6.4	4.9	5.9
La	11.4	6.45	2.9	2.4	2.9
Ce	15.4	11.7	467.8	266.3	190.4
Pr	2.28	1.46	315.9	394.6	372.5
Nd	8.89	5.50	2.8	4.5	2.4

Sm	1.73	1.11	0.4	0.4	0.4
Eu	0.377	0.341	6.2	5.0	5.6
Gd	1.54	0.984	0.2	0.1	0.2
Tb	0.221	0.155	2.0	1.7	1.8
Dy	1.35	0.953	65.4	49.6	62.9
Ho	0.298	0.203	7.6	10.8	7.7
Er	0.801	0.557	15.7	13.8	15.0
Tm	0.119	0.0831	1.1	0.9	1.1
Yb	0.744	0.549	3421.2	3832.8	3700.1
Lu	0.118	0.080	166.6	145.8	151.1

Table S 3 Retention of pollutant in WtE-BA mortars, normalized and aerated mortars

		SM	AM	0.4-Cz20S	0.55-Cz20S	0.55-Cz50S	0.55-Cz50M	0.55-Cz50C
Minor	**As**	100,0%	99,9%	100,0%	100,0%	100,0%	100,0%	100,0%
	Ba	70,0%	31,4%	78,1%	73,4%	90,4%	83,6%	86,7%
	Cd	99,9%	99,9%	99,9%	100,0%	100,0%	100,0%	100,0%
	Cr	98,8%	97,9%	98,9%	98,2%	99,5%	98,9%	99,3%
	Cu	99,8%	91,1%	97,8%	97,8%	99,8%	94,1%	96,2%
	Mg	100,0%	100,0%	100,0%	100,0%	100,0%	100,0%	100,0%
	Mo	99,0%	96,5%	98,7%	98,4%	99,4%	98,2%	98,6%
	Ni	100,0%	100,0%	99,6%	99,7%	100,0%	99,6%	99,7%
	Pb	99,9%	99,8%	99,1%	99,1%	99,8%	98,2%	95,4%
	Sb	99,8%	99,7%	99,7%	99,5%	99,7%	99,5%	99,2%
	Sn	99,8%	99,6%	99,4%	99,3%	99,5%	99,3%	100,0%
	Ti	100,0%	100,0%	100,0%	100,0%	100,0%	100,0%	100,0%
	Zn	100,0%	100,0%	100,0%	100,0%	100,0%	100,0%	100,0%
Major	**Al**	99,9%	99,9%	99,9%	99,9%	99,9%	99,9%	99,9%
	Ca	91,5%	92,1%	91,4%	91,3%	90,9%	91,8%	92,8%
	Fe	100,0%	100,0%	100,0%	100,0%	100,0%	100,0%	100,0%
	Si	100,0%	100,0%	100,0%	100,0%	100,0%	100,0%	100,0%